AJNR

Physiology of the CSF Flow-Void Sign: Modification by Cardiac Gating

Charles M. Citrin, John L. Sherman, Raymond E. Gangarosa and Diana Scanlon

AJNR Am J Neuroradiol 1986, 7 (6) 1021-1024
http://www.ajnr.org/content/7/6/1021

Physiology of the CSF Flow-Void Sign: Modification by Cardiac Gating

Charles M. Citrin[1,2]
John L. Sherman[1,3]
Raymond E. Gangarosa[4]
Diana Scanlon[4]

Low-intensity signal seen within areas of narrowing within the ventricular system has been termed the *CSF flow-void sign*. This decreased signal is related to CSF flow and turbulence. Seven normal volunteers were examined, and the changes that occurred in the appearance of the CFVS were noted when data acquisition was modified by cardiac gating. Flow-void patterns within the internal cerebral veins and basilar artery were also examined. The results of this study confirm that CSF flow is related to cardiac systole and diastole. An increase in hypointensity is seen in the areas of the aqueduct of Sylvius and the foramen of Magendie during the time at which the systemic arterial pulse wave is transmitted into the brain. The physiology of this observation is related either to a direct hydraulic effect of the venous system on the CSF or to filling and expansion of the thin-walled cerebral venous system. Hypointensity or an increase in the width of the basilar artery and internal cerebral veins during systolic data acquisition was also noted. The mechanism of this phenomenon is related to propagation of the systemic arterial pulse wave.

Recent publications and presentations [1–3] have addressed the significance of decreased signal intensity identified within the ventricular system and usually best seen at levels at which the ventricular system narrows (aqueduct of Sylvius, foramen of Magendie, and foramina of Monro). This area of decreased signal related to CSF flow and turbulence has been termed the *CSF flow-void sign* (CFVS). We have investigated the presence of the CFVS within the brains of normal volunteers and have referenced the presence and intensity of the sign as it relates to the cardiac cycle. Changes in the appearance of the CFVS have also been compared with changes observed in a major intracerebral artery and major intracerebral vein.

Subjects and Methods

Multislice MR imaging examinations were obtained using a Picker Vista MR superconductive imager operating at 0.5 T. Data were acquired with 256 views and two excitations using the 2DFT method. Scans were reconstructed and interpolated to a 512 × 512 image matrix.

Six-slice spin-echo pulse sequences were performed, with excitation of selected slices in a staggered order, exciting odd-numbered slices sequentially, followed by even-numbered slices sequentially. Slices were contiguous and were 5 mm thick in all cases. Only sagittal scans were obtained in this study because of the ease of identifying anatomic structures. An echo time (TE) value of 60 msec was used in all cases. RF stimulation and all scan data acquisitions were gated to the QRS complex; therefore, repetition time (TR) was determined by the patient's R-R interval, which varied between 710 and 1000 msec. This corresponds to a heart rate of 60–84 beats/min. Seven normal volunteers were examined. Each normal volunteer was monitored with ECG leads in place. No arrhythmias were noted. Cardiac gating was performed using a fiberoptic transmitter-receiver pair and appropriate blanking circuitry to prevent cross talk between the imager and monitoring equipment. Gating was performed on every other cardiac cycle, which resulted in the TR varying from 1420 msec to 2000 msec. Each scan was obtained with a variable delay t. The time delays t_d in milliseconds between

This article appears in the November/December 1986 issue of *AJNR* and the January 1987 issue of *AJR*.

Received February 13, 1986; accepted after revision May 28, 1986.

Presented at the annual meeting of the American Society of Neuroradiology, San Diego, January 1986.

[1] Magnetic Imaging of Washington, 5550 Friendship Blvd., Chevy Chase, MD 20815. Address reprint requests to C. M. Citrin.

[2] Department of Radiology, George Washington University School of Medicine, Washington, DC 20037.

[3] Department of Radiology, Uniformed Services University of the Health Sciences, Bethesda, MD 20814.

[4] Picker International, Inc., Highland Heights, OH 44143.

***AJNR* 7, 1021–1024, November/December 1986**
0195-6108/86/0706-1021

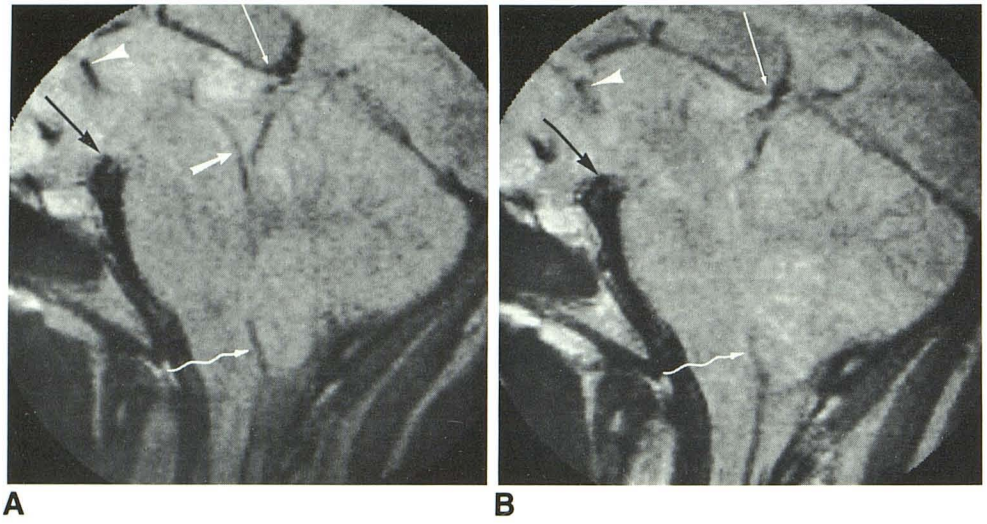

Fig. 1.—Images generated during SDA (**A**) and DDA (**B**). CFVS is seen well within aqueduct of Sylvius during SDA (**A**, *short white arrow*) and is not seen during DDA. There is diminution of CFVS within foramina of Monro during DDA (*arrowheads*). CFVS within foramen of Magendie (*wavy arrows*). Mild diminution in degree of hypointensity during DDA. Diminution in vascular flow-void sign (VFVS) within internal cerebral vein, especially at level of its junction with vein of Galen (*long white arrows*) during diastolic data acquisition, and minimal change in VFVS at tip of basilar artery (*black arrows*), with diminution in sign during DDA.

the peak of the R wave and data sampling were given approximately by $t_d = t + (k - 1)(T_{ss}/2) + TE$ for k odd and $t_d = t + (n + k - 2)(T_{ss}/2) + TE$ for k even, where t = selected time delay in msec for the first slice, k = slice number, n = number of slices = 6, T_{ss} = time between successively excited slices = 120 msec, and TE = echo time in msec.

Since the slice used was always number 3, this indicates a data acquisition delay after the R wave of 120 msec + the selected delay + TE. To obtain a CFVS that related to cardiac systole, each normal volunteer had a scan with a selected delay of 50 msec. Therefore, in all subjects a 5-mm sagittal scan was obtained with variable TR depending on the patient's cardiac rate, a TE of 60 msec, and a data acquisition delay equal to 120 msec + 50 msec + 60 msec, representing, in order, the time between successively excited slices, the selected delay, and the TE. This equals a total delay of 230 msec between the R wave and data acquisition. An additional delay was applied to the timing mechanism of the scanner so that a delay after data acquisition equal to the R-R interval would occur before initiation of any additional data acquisition. This resulted in data being acquired on every other cardiac contraction. This allowed for T2-weighting of the images, which resulted in accentuation of the CFVS and permitted easier interpretation.

A second sequence was also obtained in each subject that related to cardiac diastole. The selected time delay varied in these patients according to the patient's R-R interval. Volunteers with a slower cardiac rate had scans obtained with a selected delay as long as 750 msec, which resulted in data acquisition being obtained at a total of 930 msec after cardiac contraction; volunteers with faster rates had scans obtained with a selected delay of only 500 msec, so that data acquisition occurred at 680 msec after the R wave. The delay (t_d) was always shorter than the R-R interval. As in the systolic series, information was acquired on every other R wave.

All scans from an individual patient were imaged at the same window width and window level. The scans were then rated as to the intensity of the CFVS at the levels of the foramina of Monro, the aqueduct of Sylvius, and the foramen of Magendie. The length and width of the CFVS were also measured, using calipers to give a point-to-point length rather than following the course of curved structures such as the aqueduct of Sylvius. Comparison was also made in the degree of hypointensity and the length and width of the basilar artery and internal cerebral veins. These vascular structures were selected for comparison with the CFVS because of their midline sagittal position and simultaneous visualization of the midline CSF-containing ventricular structures.

Results

Using the parameters established above, the CFVS was noted to vary with cardiac gating. At the level of the aqueduct of Sylvius, the CFVS became much more prominent during systolic data acquisition (SDA) in six of seven volunteers (Figs. 1–3) when compared with images generated during diastolic data acquisition (DDA). At the aqueduct, the CFVS was unchanged in one volunteer. The length or width of the CFVS at the aqueduct increased in seven of seven volunteers during SDA. This resulted in demonstration of the posterior third ventricle in six volunteers and demonstration of the proximal fourth ventricle in one volunteer during SDA (Fig. 2); findings not apparent during DDA. At the foramina of Monro, the CFVS was observed in two subjects during SDA (Fig. 1) and was not present during DDA. Enhancement of the CFVS was noted in one volunteer during SDA in the mid–fourth ventricle (not shown). The other area of striking change occurred at the level of the foramen of Magendie. In six of seven subjects the CFVS became more prominent during SDA than DDA, and it was unchanged in one subject. The length and width of the CFVS were increased at the level of the foramen of Magendie in five subjects during SDA and were unchanged in two subjects.

Evaluation of the basilar artery and internal cerebral vein revealed an increase in the vascular flow-void sign (VFVS) in five of seven individuals within the basilar artery during SDA. In three of seven individuals the VFVS in the basilar artery was of greater length or width during SDA. The other subjects were unchanged when SDA was compared with DDA. Similar results occurred at the internal cerebral vein, where in four of seven individuals the VFVS was more prominent during SDA and was seen to be of either greater length or greater width in two of seven individuals (Figs. 1 and 2). The other subjects were unchanged in this category when SDA was compared with DDA.

Discussion

CSF, a plasma ultrafiltrate, is continuously formed at a rate of about 25 ml/hr. Choroidal and ependymal CSF production

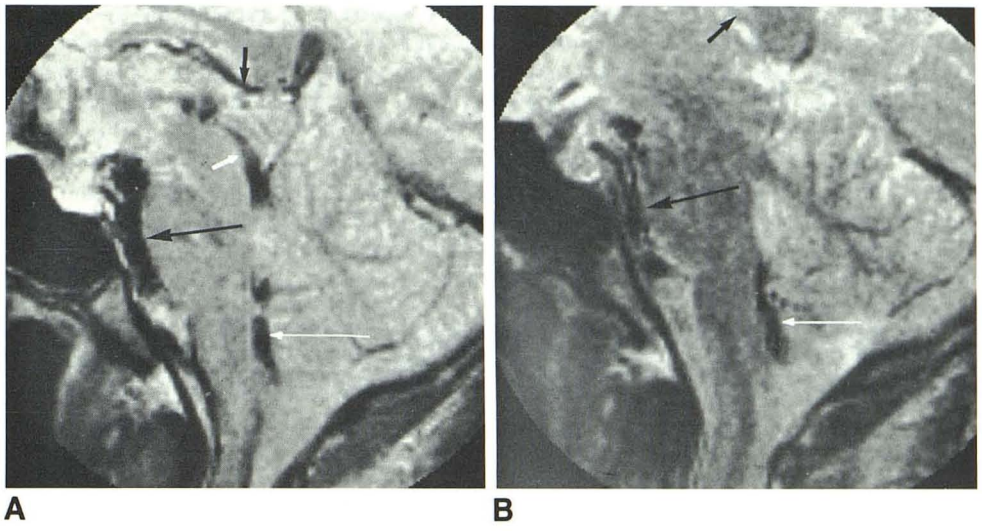

Fig. 2.—During SDA (**A**) CFVS is prominent in posterior third ventricle and aqueduct of Sylvius (*short white arrow*) and is not seen during DDA (**B**). Hypointensity within foramen of Magendie (*long white arrows*) during SDA is much wider and more hypointense than during DDA. Internal cerebral vein is seen well during SDA as a negative signal (*short black arrows*) and is barely visible during DDA. Basilar artery is much more hypointense during SDA than during DDA (*long black arrows*). Flow-void sign is not present at either foramen of Monro.

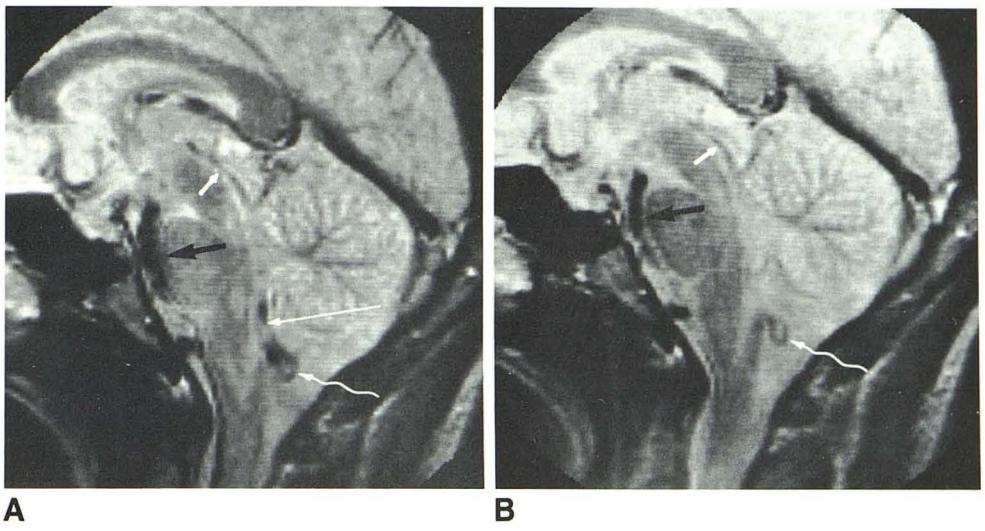

Fig. 3.—Greater hypointensity within aqueduct of Sylvius during SDA (**A**) than during DDA (**B**), and length of CFVS in aqueduct is increased during SDA (*short white arrows*). VFVS within basilar artery is increased during SDA when compared with DDA (*black arrows*). At level of foramen of Magendie, CFVS is quite prominent during SDA (*long straight white arrow*) and is not apparent during DDA. Curvilinear signal during SDA beneath foramen of Magendie (*wavy arrows*) is diminished in both width and hypointensity during DDA; this is thought to represent a loop of posterior inferior cerebellar artery.

within the ventricular system and CSF resorption by the arachnoid villi over the convexities result in a bulk CSF flow from within the ventricular system to outside the ventricular system [4, 5]. The rate of this flow is insufficient to cause signal dropout. However, vigorous pulsations of the CSF result from the action of the systolic arterial pressure pulse wave that is transmitted from the aortic root into the cerebral vasculature. The pulse wave is transmitted intact through the arteriolar and capillary arborization into the cerebral venous system and can be detected within the superior sagittal sinus [6]. This pulse wave is transmitted into the CSF. Marmarou et al. [7] contend that there is a direct hydraulic coupling of the craniospinal venous system to the CSF system. Pressure wave variations within the CSF are therefore linked by a fluid/fluid interface. Portnoy et al. [6] hypothesize that transmission of the arterial pulse wave through the capillaries into the venous system results in expansion of the thin-walled venous system. This expansion results in a pressure effect upon the brain and subsequent propagation of this pressure wave into the CSF. This is further contributed to by arteriolar and capillary filling.

After the R wave of the QRS complex, there is a delay of about 90 msec during which isometric ventricular contraction occurs [8]. After opening of the aortic valve, maximum pressure within the aorta is realized about 150 msec after the R wave. This results in dilatation of this vessel. It is the distensibility of the aorta and other arterial structures that allows for rapid propagation of the pressure pulse wave into the arterial system. The transmission of the pressure pulse wave into the carotid arteries and brain is much more rapid than that of the actual motion of blood. The pulse wave within the aorta progresses at a rate of about 5–6 m/sec, while blood flow is traveling at a rate of only 0.5 m/sec. In smaller vessels, due to a decrease in distensibility, the rate of pulse propagation may rise to 40 m/sec [9]. Concomitant with a decrease in distensibility and a rise in the rate of pulse propagation is a diminution in the amplitude of the pulse. However, there is ultimate transmission of this pulse into the arteriolar and capillary system of the brain, as well as into the cerebral venous system. The phenomenon of pulse propagation, as

opposed to actual blood flow, requires about 240 msec to be transmitted from the initiation of isometric contraction of the heart to observation at the capillary venous junction of the brain [10].

Transmission of the arterial pulse pressure wave to the brain has already occurred by the time ventricular systole has ended, about 280 msec after the R wave. Diastole follows immediately afterward and results in a prompt drop-off in pulse pressure within the carotid arteries and brain. The rate of drop-off of arterial pressure is less than that of the rapid rise during systole, but by 550 msec after the R wave in an individual with a pulse of 75 beats/min, pulse pressure has returned to presystolic levels. It remains at this lower level until the next ventricular contraction.

Comparison of systolic and diastolic gated images obtained in this study demonstrates a definite change in the CFVS. There is a clear increased presence of the degree and size of the CFVS during systole. The change is most marked in the areas of maximal narrowing of the CSF pathways, the aqueduct of Sylvius, and the foramen of Magendie, and is noted to be less prominent in areas of lesser narrowing, such as the foramina of Monro and proximal fourth ventricle. The VFVS seen within the basilar artery and internal cerebral vein also varies with systole and diastole, and is statistically almost as striking as the changes in the CFVS observed within the narrowest portions of the CSF pathways.

The effects of flow on MR images have been described [11–13]. Changes in the MR images secondary to flow have been related to both time-of-flight effects as well as spin-phase shift effects. Signal dropout perceived as the CFVS is probably related to a combination of both these effects. The spin-phase effects occur either in the imaging plane or through the imaging plane and may be perceived on transverse, coronal, or sagittal images. Pulsatile, turbulent flow will result in spin-phase effect change due to spatial variation of the spins. The appearance of the CFVS is probably not related to the phase-encoding gradient because of the strength of that gradient, which for most views is weaker than the read-out gradients. Others have offered more technical explanations of time-of-flight and spin-phase effects [14].

Regardless of the physical etiology of the CFVS, we have demonstrated that there is a clear relation between cardiac systole and the presence and enhancement of the CFVS. We attribute this to transmission of the systemic artery pulse wave into the cerebral arterial system, with propagation of that pulse wave into the cerebral venous network. The CFVS is a normal physiologic phenomenon that should not be construed as representative of pathology. Its absence, however, may be indicative of an obstructive lesion and in some instances, as a later report will demonstrate, can be pathognomonic of an obstructive lesion within the ventricular system.

REFERENCES

1. Sherman JL, Citrin CM. Magnetic resonance demonstration of normal CSF flow. *AJNR* **1986**;7:3–6
2. Citrin CM, Sherman JL. Alteration of the MRI appearance of CSF flow by cardiac gating. Presented at the annual meeting of the American Society of Neuroradiology, San Diego, January **1986**
3. Bergstrand G, Berstrom M, Nordell B, et al. Cardiac gated MR imaging of cerebrospinal fluid flow. *J Comput Assist Tomogr* **1985**;9:1003–1006
4. Milhorat TH. The third circulation revisited. *J Neurosurg* **1975**;42:628–645
5. Cutler RW, Page L, Galicich J, Waters GV. Formation and absorption of cerebrospinal fluid in man. *Brain* **1968**;91:707–719
6. Portnoy HD, Chopp M, Branch C, Shannon MB. Cerebrospinal fluid pulse waveform as an indicator of cerebral autoregulation. *J Neurosurg* **1982**;56:666–678
7. Marmarou A, Shulman K, Rosende RM. A nonlinear analysis of the cerebrospinal fluid system and intracranial pressure dynamics. *J Neurosurg* **1978**;48:332–344
8. Ganong WF. *Review of medical physiology*, Los Altos, CA: Lange Medical, **1973**
9. McDonald DA. *Blood flow in arteries*. Baltimore: Williams & Wilkins, **1974**
10. Wright S. *Applied physiology*, 11th ed. New York: Oxford University, **1965**
11. Bradley WG, Waluch V. Blood flow: magnetic resonance imaging. *Radiology* **1985**;154:554–560
12. Bradley WG, Waluch V, Laie K, Fernandez EJ, Spalter C. The appearance of rapidly flowing blood on magnetic resonance images. *AJR* **1984**;143:1167–1174
13. Mills CM, Brant-Zawadzki M, Crooks LE, et al. Nuclear magnetic resonance: principles of blood flow imaging. *AJNR* **1983**;4:1161–1166, *AJR* **1984**;142:165–170
14. Von Schulthees GK, Higgins CB. Blood flow imaging with MR: spin-phase phenomenon. *Radiology* **1985**;157:687–695